A&A 376, 820–824 (2001)
DOI: 10.1051/0004-6361:20011036

Astronomy & Astrophysics

Planetary nebula candidates in a southern region of M 33⋆

L. J. Corral[1] and A. Herrero[1,2]

[1] Instituto de Astrofísica de Canarias, c/Vía Lactea s/n, 38205 La Laguna, Spain
e-mail: ahd@ll.iac.es
[2] Departamento de Astrofísica, Universidad de La Laguna, Avda. Astrofísico Francisco Sánchez, s/n, 38071 La Laguna, Spain

Received 24 August 2000 / Accepted 11 July 2001

Abstract. In a search for emission line objects made in a southern region of M 33 using narrow band filters centered on [O III], Hα and adjacent continua, we detect some known and new objects that can be classified as planetary nebulae candidates (PNc). This search, the deepest one made up to now in M 33, has allowed us to detect 48 PNc, from which 14 have a ratio of [O III]-to-Hα fluxes greater than 1. We compare our findings with a previous search and present the list and finding charts of these interesting objects.

Key words. planetary nebulae: general – galaxies: individual: M 33

1. Introduction

Planetary nebulae (PNe) represent one of the final stages in the evolution of low and intermediate mass stars. They have been used to trace the chemical evolution of galaxies, not only in the Milky Way (see Esteban & Peimbert 1995 and references therein) but also in close neighbours such as the LMC (Dopita et al. 1997), M 31 (Richer et al. 1999; Jacoby & Ciardullo 1999) and M 32 (Richer et al. 1999). Extragalactic PNe have also been used as secondary distance indicators by means of the so–called planetary nebulae luminosity function (PNLF, see Jacoby 1997, and references therein). For this technique, complete samples of PNe up to a given magnitude are an important requirement, not the least of these being for defining the actual form of the PNLF (see Méndez 2000).

Recently Magrini et al. (2000) announced the detection of 134 candidate planetary nebulae (PNc) in M 33. This galaxy has received recent attention because, as stated by Magrini et al. (2000), it is one of the important members of the Local Group for which the PN population was poorly known. In that paper the objects were detected in Hα, [O III] and continuum images. Since we have acquired similar images in a deeper search made by us for LBV candidates in a restricted region of M 33, we report on the PNc we have found and compare the PNc reported by Magrini et al. (2000) with the sources detected by us. While our search is limited to a smaller spatial area, we should detect fainter PNc.

We find that we recover all of the PNc reported by Magrini et al. (2000) in the region observed by us, but also find new objects with similar characteristics, i.e. strong emission in Hα or [O III] and lack of emission in the continuum filter images. In order to contribute to the study of these objects in M 33 we present here the results of the search.

2. Observations

We observed 3 overlapping $\sim 6.5' \times 6.5'$ areas (see Fig. 1) in the southern arm of M 33 with the 2.5 m Nordic Optical Telescope (NOT) on La Palma. We used ALFOSC in direct image operating mode and with filters that isolate the Hα and [O III] 5007 Å lines, as well as the adjacent continuum regions. The characteristics of the filters used are presented in Table 1.

We usually take three images of the same field in order to eliminate cosmic rays and obtain deeper images after addition. In Table 2 we present the observations log, integration times and filters used.

The sky conditions were good and the seeing was better than $1''.2$ during the whole run. As its detector, ALFOSC has a $2k \times 2k$ CCD with 15 μm-wide pixels, so that the spatial scale of the images is $\sim 0''.2$/pixel.

At the beginning and end of each night we took images of the spectrophotometric standard stars BD +28 4211, Feige 110 and G191-B2B with the same filters. The standards belong to the catalogue by Oke (1990), with magnitudes corrected by Colina & Bohlin (1994) and the

Send offprint requests to: L. J. Corral,
e-mail: lcorral@ll.iac.es

⋆ Figures 3 to 11 are only available in electronic form at http://www.edpsciences.org

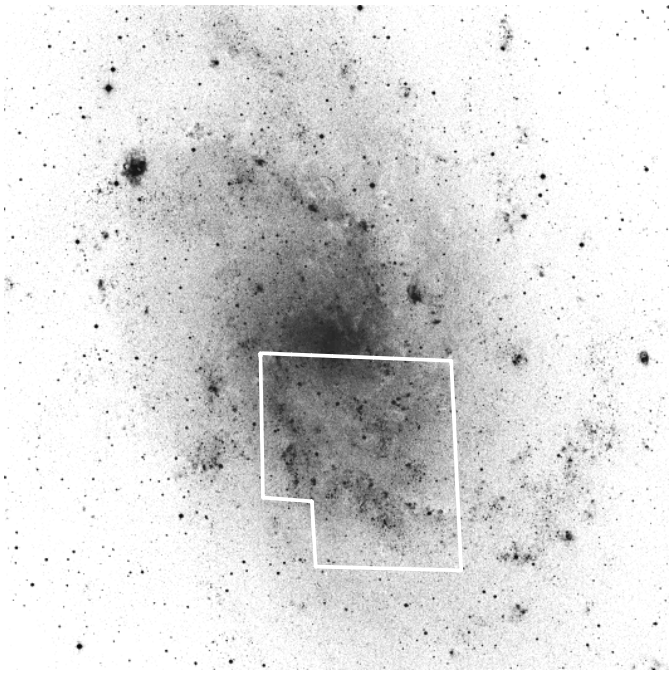

Fig. 1. The observed area of the southern arm of M 33 is outlined over a NGS-POSS image of the galaxy. The orientation of the image is N up and E to the left.

Table 1. Filters used in the observations. Given are central wavelengths and half widths at half maximum in nanometers, the peak transmission and the identification used by the NOT.

Name	λ_c nm	*FWHM* nm	T max. %	NOT ident.
[O III]	501.0	4.3	60	NOT 40
Blue cont.	521.4	10.5	77	NOT 67
Hα	656.4	3.3	66	NOT 21
Red cont.	678.8	4.5	73	NOT 54

transformation from magnitudes to fluxes by Hamuy et al. (1992). All the data can be found in Walsh (1998). We used these images to calibrate the observations of M 33.

3. Image reduction

The images were reduced with IRAF in the standard way (bias subtraction, flat-field correction and cosmic ray removal). We usually took three consecutive images of the same field in each filter (see Table 2). About 20 stars in the field were used as control points to calculate and correct the geometric distortion between images of the same field. We found that there were small shifts in the consecutive images, even though we did not move the telescope between them and used the same guide star in both images. This can be explained by mechanical flexures and torsions in the instrument, by atmospheric refraction, or by a combination of both. The images of the same field and filter were added together after correction of these shifts to obtain deeper images.

We subtract the continuum images from the on-line images in order to isolate the emission objects and areas. For this operation we scale the on-line images to account for the differently filter bandwidth, system throughput and stellar fluxes as function of wavelength.

We used the observations of the standard stars to find the scale factor between the continuum and on-line images. The scale factors obtained are 0.72 for the Hα observations and 0.38 for the [O III] images.

However, the standard stars that we observed are high temperature objects (BD+28 4211, Op; Feige 110, DOp; G191 B2B, DA0). In a galaxy like M 33 we will find very different stars, and in principle each has a different scale factor. If we then assume a single scale factor to equalize on- and off-line images we perhaps include some false emission objects that were not properly subtracted.

As an example, consider the use of black bodies from 5000 to 50 000 K and the tabulated response of the filters we use. The [O III/blue continuum] ratio would vary from 0.34 to 0.40 [1] and the [Hα/red continuum] ratio would go from 0.74 to 0.82, a ∼12 and ∼15%, respectively. Using the Strömgren y filter as continuum would result in ratios of 0.19−0.29 for [O III/y] and 0.16−0.08 for [Hα/y]. These are variations of ∼35% and 100%. These numbers illustrate nicely the importance of choosing a continuum filter close to the line wavelength and give us an idea about the possible range of variations of the scale factors.

Therefore we used ∼10 stars in each observed field to check that the scale factors found with the standard stars are not biased. We first matched the PSF of the stellar images with the IRAF task PSFMATCH and check that these test stars were not in evident emission regions. The average [Hα/red continuum] ratio found was 0.72 ± 0.02 for regions II and III (note that black bodies do not account for the stellar absorption lines). For region I the ratio was 0.47 ± 0.1, because in this case we added together only two images instead of three (see Table 2). The [O III/blue continuum] ratio found was 0.38 ± 0.06 for all images. The small variation in the average of the scale factors reflects the fact that the chosen continuum regions are close to the observed emission lines and that the difference in emission in the spectral regions observed are not too high. The possibility that by chance all our test objects have similar spectral characteristics is rulled out, because the color of these objects in our continumm images (i.e. the difference in magnitude between our blue and red continua), span almost 2 mag. We conclude that for the combination of continuum and on-line filters that we used the application of a single scale factor was safe (within the quoted errors).

We also used the images of the spectrophotometric standard stars acquired during the run to calibrate

[1] We did not apply any correction for the response of the CCD plus optics, nor for the extinction by the atmosphere. We convolve the black body emission with the spectral response of the filters used in this work that appears in the NOT web pages.

Table 2. Observations. The M 33 fields are identified as M 33 I, II and III. The field centres are given for epoch J2000.0.

Object	Filter	Int. time (s)	Date	Object	Filter	Int. time (s)	Date
BD +28 4211	Hα	60(×4)	21/X/1998	BD+ 28 4211	Hα	60(×4)	22/X/1998
	Red cont	45(×4)			Red cont.	60(×4)	
	[O III]	45(×4)			[O III]	45(×4)	
	Blue cont.	20(×4)			Blue cont.	20(×3)	
M 33 I	Blue cont.	600(×3)		Feige 110	Red cont.	60(×3)	
1:33:50 30:35:30	[O III]	600(×3)			[O III]	60(×3)	
	Red cont.	600(×3)			Blue cont.	60(×3)	
	Hα	600(×2)			Hα	60(×3)	
M 33 II	Hα	600(×3)		M 33 III	Hα	600(×3)	
1:33:38 30:35:28	Red cont.	600(×3)		1:33:38 30:32:26	Red cont.	600(×3)	
	[O III]	600(×3)			[O III]	600(×3)	
	Blue cont.	600(×3)					
				G191-2B2	Hα	25(×4)	
M 33 III	Blue cont.	600(×3)			Blue cont	25(×3)	
1:33:38 30:32:26					[O III]	25(×3)	
G191-2B2	Blue cont.	25(×4)			Red cont.	25(×3)	
	[O III]	25(×4)					
	Red cont.	25(×4)					
	Hα	25(×4)					

the M 33 images in flux. The standard star images were reduced with IRAF in the standard way and the integrated fluxes (in counts) were found with APPHOT. The published spectrophotometric measurements were convolved with the transmission function of the filters. We scaled the counts s^{-1} with the integrated flux and found the conversion factors. These conversion factors were applied to the aperture photometry of the detected emission objects (also obtained with APPHOT) giving the fluxes reported in Table 3. We did not apply any extinction correction to the fluxes that we obtain, neither by atmospheric nor galactic nature. The atmospheric extinction differs in each individual image. Taking a "average" extinction curve and the "average" air mass of the images used, we can estimate that the Hα images have an atmospheric extinction of ∼0.06 mag and the extinction of the [O III] images is ∼0.14 mag. This fact should be taken into account when comparing our results with other fluxes reported.

The positions of the sources were computed using selected isolated stars measured with APM. We obtain a solution with typical errors in the position of the order of 0.″3. To check the astrometric solution that we obtained we found in our images the position of OB (Massey et al. 1995) and WR stars (Massey & Johnson 1998) reported in the literature. We found a good correlation when we compared these with the finding charts of the objects.

4. Results

At the distance of M 33 (840 kpc, Freedman et al. 1991) and with a typical seeing of 1.″0, we expect our observed PN candidates to appear as point sources, with strong emission in Hα and [O III]λ5007 and no counterpart in the continuum regions (unless the central star is very luminous or is a binary, or unless the position of the M 33 PNe coincide with foreground stars).

We found 48 objects with these characteristics (presented in Table 3). In the first column we give the identification and the J2000.0 coordinates are presented in Cols. 2 and 3. The Hα and [O III] integrated fluxes (in units of 10^{-15} erg cm^{-2} s^{-1}) are presented in Cols. 4 and 5. In Col. 6 we give the $m(5007)$ magnitudes, derived from the expression by Jacoby (1989), $m(5007) = -2.5 \log F(5007) - 13.74$, where $F(5007)$ is the flux given in Col. 5. Finally, in Cols. 7 and 8 we give the identification of the sources in the list of PNc and the $m(5007)$ reported by Magrini et al. (2000) with the corrected coordinates reported in Magrini et al. (2001).

Using the relationship between S/N ratio and completeness given by Ciardullo et al. (1987) we obtain a limit of $m(5007) = 23.7$ for the sample. However, we have made no attempt to study the PNLF because it is clear that our sample is contaminated with compact H II regions. Twenty objects only show emission in Hα, and 14 more have $R = [\mathrm{O\,III}]/(\mathrm{H}_\alpha) < 1$ (this can be also appreciated in the way that our PNc follow the spiral arms). The other 14 objects have $R > 1$ and are then bona fide PNc. The comparatively large contamination can be understood because we are in a region of strong Hα emission (remember that our original purpose was to look for young objects, such as LBVs). Note however that we identify all objects detected by Magrini et al. (2000) in this region. As can be seen in Table 3 and Fig. 2 our derived [OIII] magnitudes for these objects differ from those reported by Magrini et al. (2000), and also their Hα fluxes tend to be larger than ours

Table 3. Candidate planetary nebulae in the southern arm of M 33. Coordinates are for epoch J2000.0, and fluxes are in units of 10^{-15} erg cm^{-2} s^{-1}.

M 33 PNc	RA	Dec	Hα Flux	[O III] Flux	m[O III]	Name Magrini	m[O III] Magrini
1	1:33:27.8	30:34:28.7	1.23	1.41	23.4	40	22.2
2	1:33:28.5	30:37:45.4	0.55	1.66	23.2	39	22.2
3	1:33:30.1	30:32:36.4	1.10				
4	1:33:30.7	30:31:39.2	2.72				
5	1:33:31.4	30:37:20.5	3.14				
6	1:33:31.9	30:30:32.4	1.10	1.60	23.3	45	22.5
7	1:33:32.2	30:31:46.0	2.47	0.95	23.8		
8	1:33:32.7	30:32:08.3	3.47				
9	1:33:33.2	30:37:34.3	2.35	2.21	22.9		
10	1:33:33.8	30:32:15.2	4.72				
11	1:33:33.8	30:32:58.8	0.78				
12	1:33:34.2	30:32:45.2	1.72				
13	1:33:34.6	30:37:00.6	3.19				
14	1:33:34.9	30:32:24.3	0.43				
15	1:33:35.3	30:32:53.6	7.24	0.63	24.3		
16	1:33:36.2	30:35:19.9	0.79				
17	1:33:36.8	30:31:40.4	0.26	1.41	23.4	48	23.18
18	1:33:37.8	30:33:52.1	0.89	0.49	24.5		
19	1:33:37.9	30:32:05.5	1.47				
20	1:33:38.6	30:33:01.9	0.76	1.94	23.0	51	22.4
21	1:33:40.2	30:37:48.8	1.12	2.53	22.8		
22	1:33:42.3	30:37:17.1	1.49				
23	1:33:42.3	30:37:38.6	1.40	2.73	22.7	54	21.65
24	1:33:43.4	30:35:24.7	1.86	0.42	24.7		
25	1:33:43.8	30:33:26.0	0.44	1.46	23.4		
26	1:33:44.3	30:36:22.2	10.24	0.47	24.6		
27	1:33:47.3	30:37:10.7	6.42				
28	1:33:48.3	30:33:15.1	2.23	2.30	22.9		
29	1:33:48.6	30:35:47.6	1.38	4.08	22.2	62	21.73
30	1:33:49.4	30:32:05.6	0.91	3.30	22.5	65	21.87
31	1:33:49.4	30:32:27.5	1.54	0.59	24.3		
32	1:33:50.9	30:33:43.2	1.18				
33	1:33:50.9	30:37:10.5	3.74			66	23.56
34	1:33:51.4	30:35:50.7	11.03	1.12	23.6		
35	1:33:51.8	30:32:59.7	1.85				
36	1:33:52.2	30:36:03.6	1.63				
37	1:33:52.5	30:33:59.1	1.02				
38	1:33:52.7	30:37:37.7	2.37	7.74	21.5	68	20.99
39	1:33:53.1	30:34:00.5	4.23				
40	1:33:53.6	30:33:23.5	2.77	0.93	23.8		
41	1:33:54.7	30:36:05.1	2.14	4.33	22.2	69	21.78
42	1:33:54.9	30:37:44.0	6.80	0.94	23.8	70	24.00
43	1:33:55.7	30:34:53.6	0.85				
44	1:33:57.1	30:36:46.9	0.79	2.97	22.6	73	22.13
45	1:33:57.6	30:32:23.1	1.01	0.46	24.6		
46	1:33:58.4	30:36:23.7	2.70	1.07	23.7		
47	1:33:58.7	30:34:59.6	5.39	2.21	22.8		
48	1:33:59.4	30:34:51.2	3.20	0.64	24.2		

for objects in common. This discrepancy can be partly attributed to the fact that we do not correct for extinction, and to the slightly poorer seeing conditions, the larger spatial scale of the images and the use of the Strömgren y filter as continuum in the Magrini et al. (2000) observations.

Taking all these problems into account we think we have to wait for follow-up spectroscopy and confirmation of the PN nature of the candidates before going on to work with the PNLF.

Finding charts for the PNc found in this paper are shown in Figs. 3 to 11. We present the Hα- and [O III]-subtracted images in the upper part of the panel and the red and blue continuum images in the lower part of the panels. The PNc are marked with a circle and the

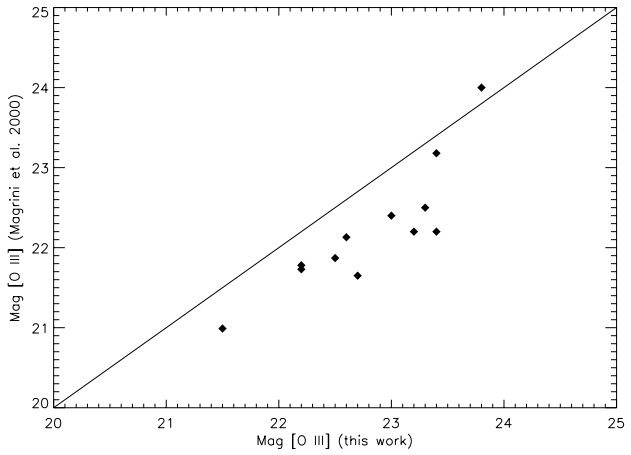

Fig. 2. Comparision of [O III] magnitudes for objects in common with Magrini et al. (2000). Our measurements tend to be fainter than those of Magrini et al. (2000) by about 0.6 mag in average.

horizontal bar is $\sim 10''$ long. The orientation of the images is N up and E to the left.

5. Conclusions

We use the method of subtracted images to identify PNc candidates as those objects with emission in Hα or [O III] lines, but with a lack of emission in the continuum filter images. We find that the uncritical use of a single scale factor may introduce errors comparable to those of other error sources even when using continuum filters close to the on-line filters and that these errors increase with the separation in wavelength between on-line and continuum filters.

We find 48 sources that fulfill the criteria given above and comparing our results with those of a previous search by Magrini et al. (2000, 2001) we found good agreement in the objects detected, but we derive smaller fluxes.

Following the criterion that those objects with an [OIII]/Hα ratio greater that 1.0 are bona fide PNe, we find 14 such objects in the area searched, 4 of them had not been reported before. The rest are probably either low excitation PNe or small H II regions. A spectroscopic follow-up study is needed to find the true nature of the sources.

Acknowledgements. LC acknowledges a CONACyT (México) posdoctoral grant at the IAC. AH acknowledges support for this work from the Spanish DGES under project PB97-1438-C02-01 and from the Gobierno Autonómico de Canarias under project PI1999/008. The data presented here have been taken using ALFOSC, which is owned by the Instituto de Astrofísica de Andalucía (IAA) and operated at the Nordic Optical Telescope under agreement between IAA and the NBIfA of the Astronomical Observatory of Copenhagen.

References

Ciardullo, R., Ford, H. C., Neill, J. D., et al. 1987, ApJ, 318, 520
Colina, L., & Bohlin, R. C. 1994, AJ, 108, 1931
Dopita, M., Vassiliadis, E., Wood, P. R., et al. 1997, ApJ, 474, 188
Esteban, C., & Peimbert, M. 1995, RMxAAC, 3, 133
Freedman, W. L., Wilson, C. D., & Madore, B. F. 1991, ApJ, 372, 455
Hamuy, M., Walker, A. R., Suntzeff, N. B., et al. 1992, PASP, 104, 533
Jacoby, G. H. 1989, ApJ, 339, 39
Jacoby, G. H. 1997, in Planetary Nebulae, ed. H. J. Habing, & H. J. G. L. M. Lamers (Kluwer, Dordrecht), IAU Symp., 180, 448
Jacoby, G. H., & Ciardullo, R. 1999, ApJ, 515, 169
Magrini, L., Corradi, R. L. M., Mampaso, A., & Perinotto, M. 2000, A&A, 355, 713
Magrini, L., Cardwell, A., Corradi, R. L. M., Mampaso, A., & Perinotto, M. 2001, A&A, 367, 498
Massey, P., Armandroff, T., Pyke, R., Patel, K. & Wilson, C. D. 1995, AJ, 110, 2715
Massey, P., & Johnson, O. 1998, ApJ, 505, 793
Méndez, R. H. 2000, in The VLT Opening Symp. 242, ed. J. Bergeron, & A. Renzini, Proc. of the ESO Symp. held at Antofagasta, Chile, 1–4 March, 1999 (Springer-Verlag)
Oke, J. B. 1990, AJ, 99, 1621
Richer, M. G., Stasinska, G., & McCall, M. L. 1999, A&AS, 135, 203
Walsh, J. 1998, in `http://www.eso.org/observing/standards/spectra`